Available online at www.sciencedirect.com

ScienceDirect

Ceramics International 40 (2014) 3747–3753

CERAMICS INTERNATIONAL

www.elsevier.com/locate/ceramint

Influence of synthesis conditions on the microstructure of Li–Ta–Ti–O microsheets by molten salt method

Zhiqiang Zhang[a,b], Zhifu Liu[a,*], Yongxiang Li[a,**]

[a]CAS Key Lab of Inorganic Functional Materials and Devices, Shanghai Institute of Ceramics, Chinese Academy of Sciences, Shanghai 200050, PR China
[b]The University of Chinese Academy of Sciences, Beijing 100049, PR China

Received 9 August 2013; received in revised form 12 September 2013; accepted 12 September 2013
Available online 20 September 2013

Abstract

M-phase Li–Ta–Ti–O (LTT) microsheets were synthesized by the molten salt method. Scanning electron microscopy, X-ray diffraction, transmission electron microscopy, and electron diffraction analyses were performed to analyze the morphology and microstructure of the LTT microsheets. The average number of layers of the LTT microsheets increases with increasing the synthesis temperature and holding time, and pure M-phase LTT microsheets are obtained at a temperature above 1000 °C. Both terrace-ledge-kink and Ostwald ripening mechanisms are important for the formation of the M-phase LTT microsheets. We demonstrate that the size of LTT microsheets could be controlled by adjusting the synthesis temperature, holding time, and the weight ratio of the raw powders to LiCl salt. These LTT microsheets with tunable size are promising building blocks for high performance microwave ceramics.

Keywords: Molten salt method; Synthesis conditions; M-phase LTT microsheets; Growth process

1. Introduction

Synthesizing ceramic powders with controlled composition, morphology, crystal phase, crystallinity and purity is extremely important for obtaining high performance ceramics. The traditional approach in making such materials has been the solid-state reaction process, however more recently various methods such as sol–gel [1], precipitation [2], hydrothermal synthesis [3], molten salt [4], combustion [5], thermal evaporation [6], have been applied in synthesizing a variety of ceramic systems. Highly crystalline powders can be obtained using molten salt synthesis due to the good activity of the raw materials in the molten salt solution at high synthesis temperatures. The fluidity of the molten salt also plays a key role for ion transportation required for particle growth following the crystal growth habit. As a consequence, the molten salt method has been widely adopted for the synthesis of oxides such as titanates, niobates, tantalates, in different forms such as nanoparticles [4], nanorods [7], nanowires [8], microsheets [9], plates [10], or even single crystals [11].

$Li_{1+x-y}M_{1-x-3y}Ti_{x+4y}O_3$ ($M=Nb^{5+}$, Ta^{5+}), so-called "M-phase", is a promising material for microwave dielectric components application due to its relatively low sintering temperature and tunable dielectric properties, and this tenability is achieved by changing the composition of the solid solution [12–14]. Borisevich et al. [15] confirmed the existence of the $Li_{1+x-y}Ta_{1-x-3y}Ti_{x+4y}O_3$ ($0.10<x<0.15$, $0.05<y<0.175$) M-phase solid solution with a structure analogous to $Li_{1+x-y}Nb_{1-x-3y}Ti_{x+4y}O_3$, which is a homologous series of commensurate intergrowth structures with $LiNbO_3$-type (LN) slabs separated by single $[Ti_2O_3]^{2+}$ corundum-type layers [16]. The average number of layers in the repeatable structure block can be represented by N, which is a sum of LN-type layers and $[Ti_2O_3]^{2+}$ corundum-type layers. Fig. 1 shows a polyhedral representation of M-phase $Li_{1+x-y}Ta_{1-x-3y}Ti_{x+4y}O_3$ with $N=10$ projected along [110]. The laminate structure makes the M-phase compounds tend to grow along the in-plane direction to form sheet-like grains under thermodynamically balanced conditions, e.g. the high temperature sintering and molten salt

*Corresponding author. Fax: +86 21 52413122.
**Corresponding author.
E-mail addresses: liuzf@mail.sic.ac.cn (Z. Liu), yxli@mail.sic.ac.cn (Y. Li).

0272-8842/$ - see front matter © 2013 Elsevier Ltd and Techna Group S.r.l. All rights reserved.
http://dx.doi.org/10.1016/j.ceramint.2013.09.046

synthesis [9,17]. These kind of sheet-like grains provide a framework to tune the properties of the materials through thickness and orientation of the sheet-like grains in ceramics [14,18,19]. Therefore the synthesis of morphology controlled $Li_{1+x-y}M_{1-x-3y}Ti_{x+4y}O_3$ (M=Nb^{5+}, Ta^{5+}) M-phase particles would provide excellent building blocks for fabrication high performance ceramics.

In this work, M-phase $Li_{1+x-y}Ta_{1-x-3y}Ti_{x+4y}O_3$ (LTT) microsheets were synthesized by the molten salt method. The effects of synthesis temperature, holding time and the weight ratio of raw powders to LiCl salt on the crystal structure and morphology of LTT microsheets was investigated. The growth process of the M-phase LTT microsheets is also discussed.

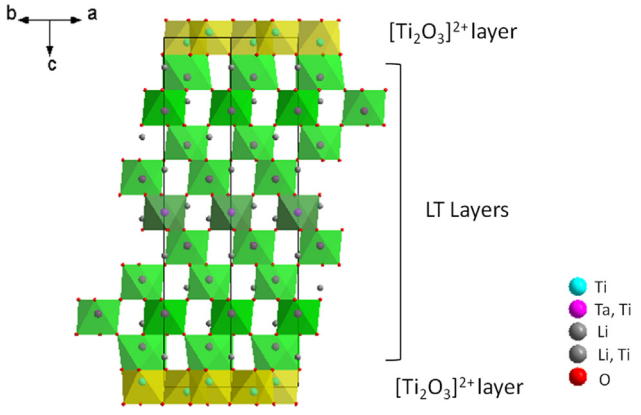

Fig. 1. Polyhedral representation of M-phase $Li_{1+x-y}Ta_{1-x-3y}Ti_{x+4y}O_3$ with $N=10$ projected along [110] (data from Ref. [16]).

2. Experimental procedure

Analytical-grade oxide powders Li_2CO_3 (98%), Ta_2O_5 (99.99%), TiO_2 (99.3%) were used as raw materials. These powders were weighted according to the nominal composition of $LiTa_{0.6}Ti_{0.5}O_3$ and mixed by ball milling in ethanol using ZrO_2 balls for 8 h, and then dried. The combined powders were mixed with LiCl (99.5%) at a weight ratio of 1:1, 1:2 and 1:3, respectively. The resultant powders were placed in a covered crucible and heated to different temperatures of 650 °C, 750 °C, 850 °C, 950 °C, 1000 °C and 1050 °C. Heat treatment was carried out for different holding times (0.5 h, 1 h, 3 h, 6 h, and 9 h). The synthesized powders were washed with de-ionized water until no Cl^- ions were detected. The crystal phases of the products were studied by X-ray Diffraction (XRD) with a Cu-$K\alpha$ radiation (D/Max-2550V, Rigaku, Tokyo, Japan). The morphology was observed by Scanning Electron Microscopy (SEM, TM-3000, Hitachi, Japan). The high resolution microstructure images, Energy Dispersive X-ray Spectroscopy (EDX), and electron diffraction patterns were studied using a JEM-2100F Transmission Electron Microscope (TEM).

3. Results and discussion

Fig. 2(a) shows the XRD patterns of the products at different synthesis temperatures and with a raw material powders/LiCl salt ratio of 1:2. The $LaTiO_3$ phase appears after heating the sample at 650 °C for only 0.5 h and the product is a mixture of $LiTaO_3$ phase (JCPDS card No. 29-0836) and TiO_2 phase

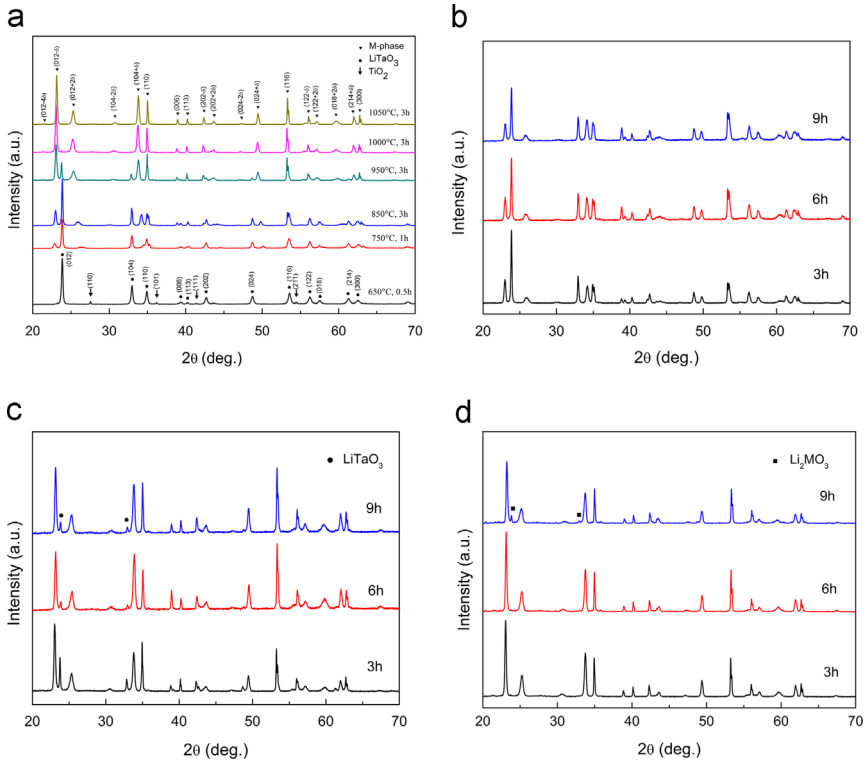

Fig. 2. XRD patterns of LTT powders prepared by molten salt synthesis with a raw powder/LiCl salt ratio of 1:2: (a) various synthesized temperatures; (b) different holding time at 850 °C; (c) different holding time at 950 °C; (d) different holding time at 1000 °C.

(JCPDS card No. 76-0649). When heated to 750 °C for 1 h, the raw material TiO_2 is no longer present and M-phase LTT appears. For the samples heated between 750 °C and 950 °C, the products are mixtures of $LiTaO_3$ phase and M-phase LTT. Pure crystalline M-phase LTT was obtained at synthesis temperatures of 1000 °C and above. Since the M-phase LTT is a homologous series of commensurate intergrowth structures with $LiTaO_3$-type (LT) slabs separated by $[Ti_2O_3]^{2+}$ corundum-type layers, the XRD pattern of M-phase LTT can be considered as the derivative of $LiTaO_3$ phase with peaks splitting. Roth and Davis introduced the fractional Miller indexes and incommensurate parameter δ to index the XRD patterns of the M-phase [20]. This method was used to index the XRD patterns of products from the molten salt synthesis. The diffraction peaks such as $(012+2\delta)$, $(104+\delta)$ and $(024+\delta)$ shifted to lower angles when synthesis temperature increased from 750 °C to 1000 °C, indicating that the amount of Ti in M-phase LTT decreased [21,22], that is to say, the average number of layers in each structure block increased. This implies that high temperature promotes the reaction of $LiTaO_3$ with Ti-rich M-phase LTT and by inserting the $LiTaO_3$ into the M-phase LTT. Finally, pure M-phase LTT was obtained by consuming the $LiTaO_3$ phase.

Fig. 2(b)–(d) show the XRD patterns of the products synthesized at 850 °C, 950 °C, 1000 °C, respectively, for different holding times (3 h, 6 h, 9 h) at a raw powder/LiCl salt ratio of 1:2. At 850 °C a small change can be observed from the XRD patterns with the increase of synthesis time, indicating the reaction was very slow due to the low temperature. At 950 °C, the amount of $LiTaO_3$ phase decreased with increasing of holding time, implying the reaction is more active at elevated temperature. The powders synthesized at 1000 °C resulted in pure M-phase for holding even only 3 h. Unexpectedly, the peaks of a second phase whose structure is similar to that of $LiTaO_3$, appeared for sample synthesized at 1000 °C for 9 h. This phenomenon was also observed in previous report [9]. Since the $LiTaO_3$ phase was exhausted at 3 h, the new phase could not be a $LiTaO_3$ phase. Farber et al. [16] reported that the central region of each LN block approaches the stoichiometry of Li_2MO_3 and has a structure similar to that of $LiTaO_3$ due to Li insertion into LT blocks. The extra XRD peaks observed from the sample synthesized at 1000 °C for 9 h may originate from the Li_2MO_3 structure formed due to the inserting excessive Li into LT blocks.

Fig. 3 shows the morphology of the products synthesized at various temperatures and for different holding times at a raw powder/LiCl salt ratio of 1:2. Only small particles are observed for sample synthesized at 650 °C for 0.5 h. XRD reveals the particles are mixture of $LiTaO_3$ and TiO_2. Microsheet morphology was observed in samples synthesized at 750 °C and above. However, there were still particle concomitants in the samples synthesized at 750 °C, 850 °C and 950 °C, yet the amount of particle contamination decreased less with increasing synthesis temperature and holding time. The size of microsheets became larger with increasing the synthesis temperature, and by extending the holding time from 3 h to 9 h, the size of microsheets also increased. The microsheets synthesized at 1050 °C for 3 h showed the largest size of about 40–60 μm in diameter and were approximately 0.9 μm thick as shown in Fig. 3(l). Fig. 3(m) is the enlarged view of Fig. 3(i), in which the microsheets exhibit a hexagonal shape, and growth step on the surface can be seen. This kind of special morphology reveals the growth habit and mechanism of the microsheets in the molten salt flux.

Fig. 4 presents the high resolution transmission electron microscopy (HRTEM) images of the microsheets synthesized at different conditions (750 °C for 1 h, 950 °C for 3 h, 1000 °C for 3 h), and the corresponding electron diffraction patterns are also shown in Fig. 4, respectively. HRTEM images show parallel fringes, revealing the layered structure of the microsheets. Furthermore, the electron diffraction patterns also exhibit periodicity. It should be noted that the HRTEM images and the diffraction patterns were measured from the cross-section of the microsheets that are perpendicular to the microsheet surface. This indicates that they have periodical layered structure along the *c*-axis. The periodicity is attributed to a LT-based superstructure with a repeatable structure block containing $(L+1)=N$ cation layers along the *c*-axis of hexagonal cell, as shown in Fig. 1. From the electron diffraction patterns we know that for the three different samples, N is equal to 7, 8 and 9. The increase of N implies that there are more LT layers between two $[Ti_2O_3]^{2+}$ corundum-type layers. Therefore we can conclude that higher temperature and longer time promote the reaction between Ti-rich M-phase LTT and $LiTaO_3$.

Fig. 5 shows the EDX spectra of the microsheets in the products synthesized at different conditions and the chemical composition data are listed in Table 1. Clearly the ratio of Ti/Ta decreases with increasing synthesis temperature and holding time. Since the M-phase LTT microsheets have layered structure composed of the LT layers and $[Ti_2O_3]^{2+}$ corundum-type layers, the Ti/Ta ratio provides indirect information of the numbers of the LT layers and $[Ti_2O_3]^{2+}$ corundum-type layers in the microsheets. The decrease of Ti/Ta ratio implies the increase of the LT layers in the periodical microstructure of the microsheets. This is consistent with the results of electron diffraction and XRD shown previously.

The effect of salt amount was also investigated. Fig. 6 shows the XRD patterns of the products synthesized at 1000 °C for 3 h at different weight ratios of raw powder to LiCl salt (1:1, 1:2, and 1:3). With the exception of the M-phase LTT, second phase diffraction peaks are observed from the XRD patterns where the ratios were 1:1 and 1:3. For the 1:1 sample, transportation of ions is slow due to high viscosity resulting from low raw materials to salt ratio, which decreased the reaction rate between $LiTaO_3$ phase and Ti-rich M-phase LTT. Therefore the second phase should be $LiTaO_3$, just as the sample synthesized below 1000 °C. At a raw material to LiCl ratio of 1:3, large amount of salt flux promoted the ion transportation and crystal phase formation. Furthermore, much more Li in ambient environment promoted the insertion process of Li into LT blocks, accelerating the formation of Li_2MO_3, which has a structure similar to that of $LiTaO_3$ [16].

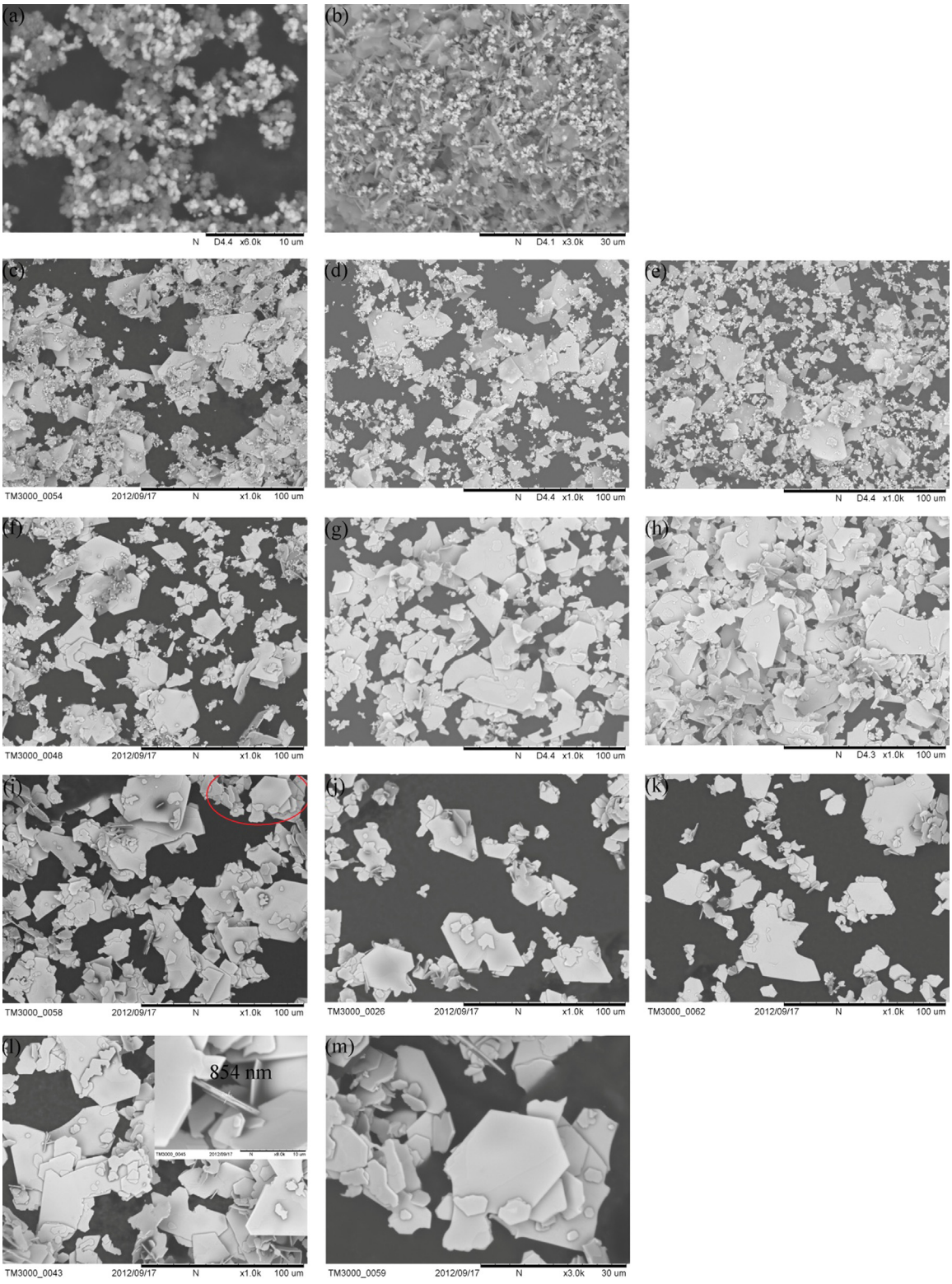

Fig. 3. SEM micrographs of LTT powders prepared by molten salt synthesis with a raw powder/LiCl salt ratio of 1:2:(a) 650 °C for 0.5 h; (b) 750 °C for 1 h; (c–e) 850 °C for 3, 6, 9 h; (f–h) 950 °C for 3, 6, 9 h; (i–k) 1000 °C for 3, 6, 9 h; (l) 1050 °C for 3 h; (m) enlarged view of (i).

This is similar to the sample synthesized at 1000 °C for 9 h as discussed above.

Fig. 7 shows the morphology of the products prepared at 1000 °C for 3 h with different salt content. When the weight ratio of raw powders to LiCl salt was 1:2, the microsheets had larger size than the other two and have more perfect morphology. More or less salt content both resulted in decrease of the size of microsheets greatly. For molten salt synthesis, the product's morphology is mainly controlled by the nucleation process and growth progress [23]. Too little salt slowed down ion diffusion and

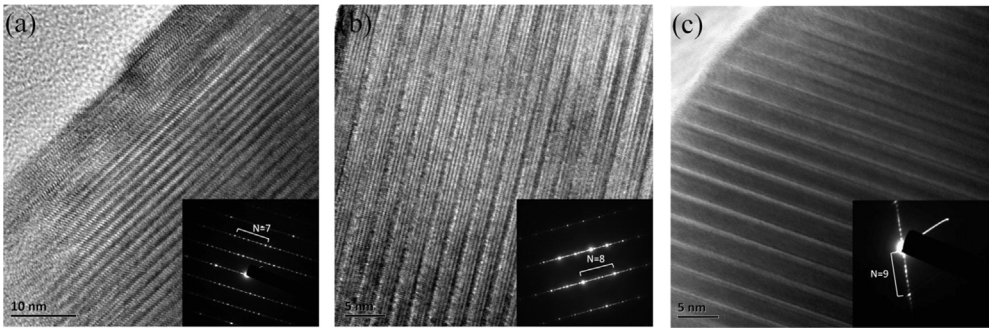

Fig. 4. HRTEM images and electron diffraction patterns of M-phase microsheets in the products synthesized at different conditions: (a) 750 °C for 1 h, (b) 950 °C for 3 h and (c) 1000 °C for 3 h.

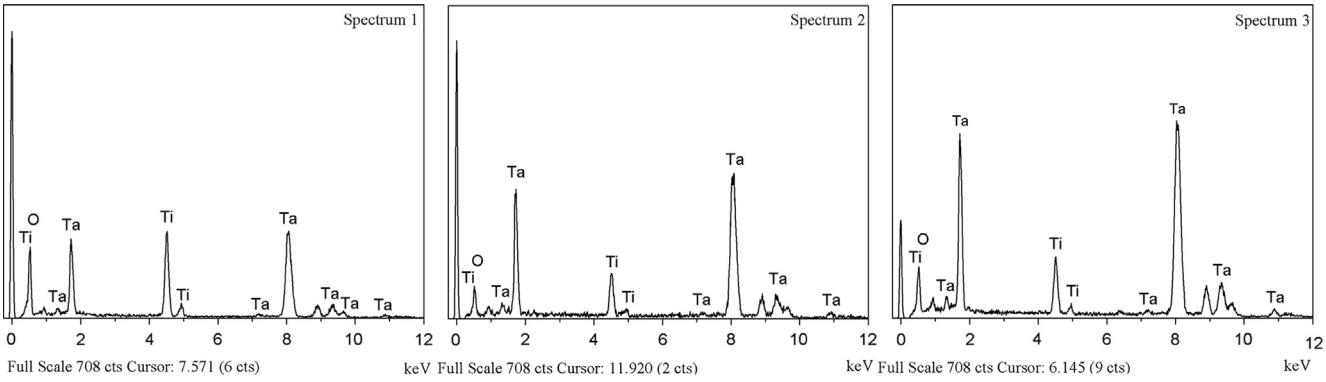

Fig. 5. EDX spectra of the microsheets in the products synthesized at different conditions (Spectrum 1: 750 °C for 1 h, Spectrum 2: 950 °C for 3 h, Spectrum 3: 1000 °C for 3 h).

Table 1
Chemical compositions data of microsheets in the products synthesized at different conditions (Spectrum 1: 750 °C for 1 h, Spectrum 2: 950 °C for 3 h, Spectrum 3: 1000 °C for 3 h).

Element	Spectrum 1		Spectrum 2		Spectrum 3	
	(wt%)	(at%)	(wt%)	(at%)	(wt%)	(at%)
O *K*	18.74	48.39	7.41	31.42	10.12	39.90
Ti *K*	52.14	44.96	32.48	46.03	29.67	39.09
Ta *M*	29.12	6.65	60.11	22.55	60.21	21.00
Ti/Ta (atom)	6.76		2.05		1.86	

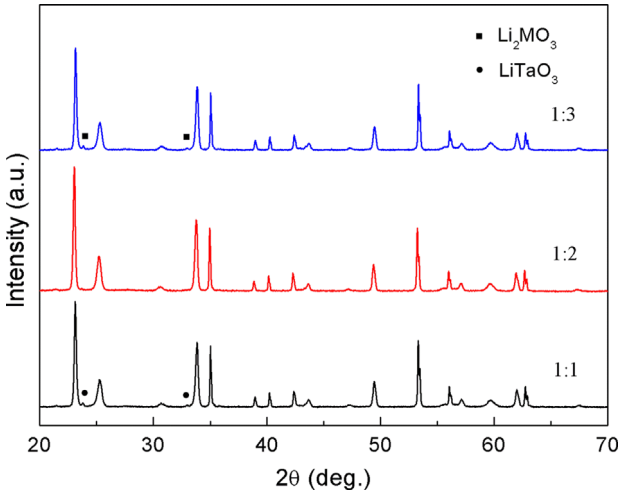

Fig. 6. XRD patterns of LTT powders prepared by molten salt synthesis at 1000 °C for 3 h with different salt contents.

transport processes which inhibited the grain growth. Too much salt diluted the raw materials and promoted the nucleation process. Both resulted in smaller size microsheets.

Based on the above experiments results, the M-phase LTT microsheets growth process is proposed in Fig. 8. At the beginning of the synthesis reaction, $LiTaO_3$ particles are formed in the LiCl flux and then Ti-rich M-phase LTT nucleate resulting from the reaction between $LiTaO_3$ and TiO_2. Since M-phase LTT belongs to the P3 space group, there is preferential growth along the in-plane direction and form hexagonal sheets morphology [16]. Moreover, the M-phase LTT can react with $LiTaO_3$ to form new M-phase LTT through the diffusion and exchange of Ti and Ta. Some new M-phase LTT nucleates in the LiCl flux and grow up alone, however, most of new M-phase LTT nucleate on the surface of M-phase LTT microsheets to form their new layers since nucleation on the microsheets surfaces is easier. Terraces come into being as a result. Due to the different relative growth rate of kink, terrace edge and surface, increasing number of M-phase LTT layers are formed and grow up via terrace-ledge-kink mechanism. The development of each layer can be divided into a number of individual growth processes including nucleation of a new layer (or terrace), growth at edges sites and kink sites [24].

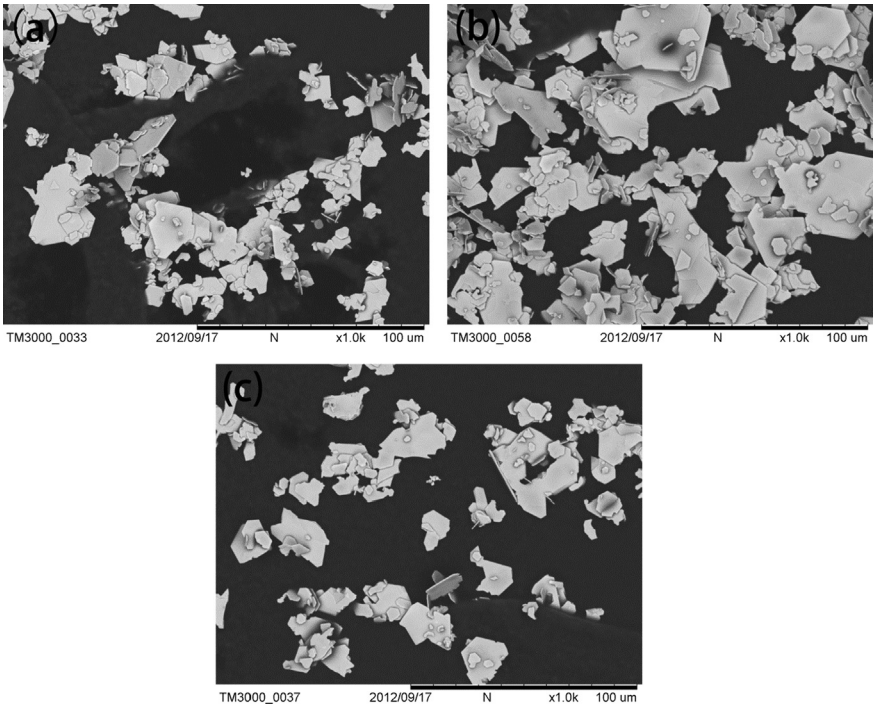

Fig. 7. SEM micrographs of LTT powders prepared by molten salt synthesis at 1000 °C for 3 h with different salt contents: (a) 1:1, (b) 1:2 and (c) 1:3.

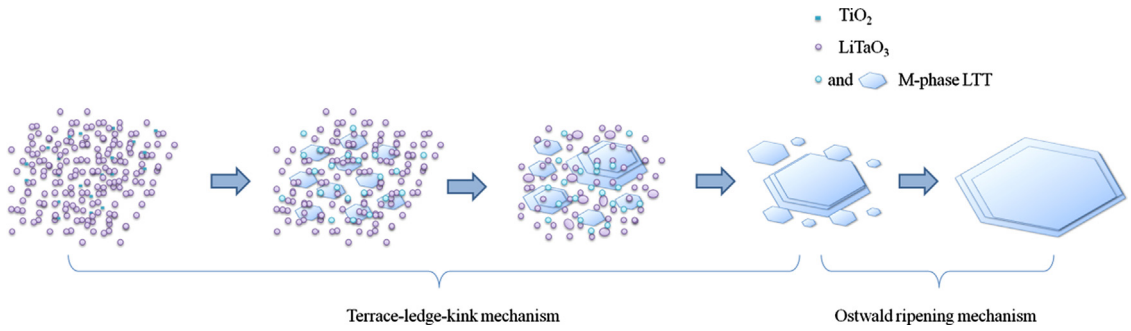

Fig. 8. Schematic diagram of the growth process of M-phase LTT microsheets.

Pure M-phase LTT microsheets form the depletion of $LiTaO_3$. After this, the M-phase LTT microsheets continue to grow up by consuming the small microsheets near them according with Ostwald ripening mechanism [23]. Usually, longer holding time is greatly helpful for the growth of microsheets according to the growth mechanism discussed above. In this work, however, much longer holding time did not result in much larger plates at 850 °C and 1000 °C or higher temperature. This is because the low temperature decreased the diffusion rate of ions, which inhibited the growth of LTT microsheets at 850 °C. At 1000 °C or higher temperature, the growth and dissolving of the microsheets may reach a dynamic balance when the microsheets grow to a certain size.

4. Conclusions

In summary, M-phase LTT microsheets with different sizes could be synthesized by the molten salt method. The synthesis temperature, holding time and the weight ratio of raw powders to LiCl salt have a large effect on the growth process of M-phase LTT microsheets and thus influence their structure and morphology. Pure M-phase LTT was obtained at temperature above 1000 °C. The average size of the LTT microsheets increases with increasing reaction temperature and holding time. When the weight ratio of raw powder to LiCl salt is 1:2, the LTT plates have larger size and more perfect morphology. Both terrace-ledge-kink mechanism and Ostwald ripening mechanism are important for the formation of the M-phase LTT microsheets. These M-phase LTT microsheets with tunable sizes can be used as building blocks for microwave dielectric ceramics and microwave components.

Acknowledgments

This work was supported by the Ministry of Sciences and Technology of China through 973 Project (2012CB619406), and The National Natural Science Foundation of China (50932007, 51172257).

References

[1] J. Li, T. Qiu, C. Fan, P. Xu, Synthesis and microwave dielectric properties of $Ca_{0.6}La_{0.267}TiO_3$ nanocrystalline powders by sol–gel method, Journal of Sol–Gel Science and Technology 59 (2011) 525–531.

[2] I. Mobasherpour, M.S. Heshajin, A. Kazemzadeh, M. Zakeri, Synthesis of nanocrystalline hydroxyapatite by using precipitation method, Journal of Alloys and Compounds 430 (2007) 330–333.

[3] F. Zhang, S. Bai, T. Karaki, Preparation of plate-like potassium sodium niobate particles by hydrothermal method, Physica Status Solidi A—Applications and Materials Science 208 (2011) 1052–1055.

[4] C. Mao, G. Wang, X. Dong, Z. Zhou, Y. Zhang, Low temperature synthesis of $Ba_{0.70}Sr_{0.30}TiO_3$ powders by the molten-salt method, Materials Chemistry and Physics 106 (2007) 164–167.

[5] S. Deka, P.A. Joy, Enhanced permeability and dielectric constant of NiZn ferrite synthesized in nanocrystalline form by a combustion method, Journal of the American Ceramic Society 90 (2007) 1494–1499.

[6] W. Khongwong, M. Imai, K. Yoshida, T. Yano, Synthesis of beta-SiC/SiO_2 core-shell nanowires by simple thermal evaporation, Journal of the Ceramic Society of Japan 117 (2009) 194–197.

[7] C.Y. Xu, L. Zhen, R. Yang, Z.L. Wang, Synthesis of single-crystalline niobate nanorods via ion-exchange based on molten-salt reaction, Journal of the American Chemical Society 129 (2007) 15444–15445.

[8] L. Li, J. Deng, J. Chen, X. Sun, R. Yu, G. Liu, X. Xing, Wire structure and morphology transformation of niobium oxide and niobates by molten salt synthesis, Chemistry of Materials 21 (2009) 1207–1213.

[9] Z. Lu, Y. Wang, W. Wu, Y. Li, Morphology and structure of $LiNb_{0.6}Ti_{0.5}O_3$ particles by molten salt synthesis, Journal of Alloys and Compounds 509 (2011) 9696–9701.

[10] Y.F. Liu, Y.N. Lu, M. Xu, L.F. Zhoun, Formation mechanisms of platelet $Sr_3Ti_2O_7$ crystals synthesized by the molten salt synthesis method, Journal of the American Ceramic Society 90 (2007) 1774–1779.

[11] J. Sun, G. Chen, Y. Li, R. Jin, Q. Wang, J. Pei, Novel (Na, K)TaO_3 single crystal nanocubes: molten salt synthesis, invariable energy level doping and excellent photocatalytic performance, Energy and Environmental Science 4 (2011) 4052–4060.

[12] A. Borisevich, P.K. Davies, Microwave dielectric properties of $Li_{1+x-y}M_{1-x-3y}Ti_{x+4y}$ (M= Nb^{5+}, Ta^{5+}) solid solutions, Journal of the European Ceramic Society 21 (2001) 1719–1722.

[13] Q. Zeng, W. Li, J.L. Shi, J.K. Guo, Microwave dielectric properties of $5Li_2O$–$0.583Nb_2O_5$–$3.248TiO_2$ ceramics with V_2O_5, Journal of the American Ceramic Society 89 (2006) 3305–3307.

[14] Z. Lu, Y. Li, Y. Wang, W. Wu, Y. Li, Anisotropic dielectric properties of $LiNb_{0.6}Ti_{0.5}O_3$ microwave ceramics by screen-printing templated grain growth, Journal of the American Ceramic Society 94 (2011) 4364–4370.

[15] A.Y. Borisevich, P.K. Davies, Synthesis and dielectric properties of $Li_{1-x+y}Ta_{1-x-3y}Ti_{x+4y}O_3$ M-Phase solid solutions, Journal of the American Ceramic Society 85 (2002) 2487–2491.

[16] L. Farber, I. Levin, A. Borisevich, I.E. Grey, R.S. Roth, P.K. Davies, Structural study of $Li_{1+x-y}Nb_{1-x-3y}Ti_{x+4y}O_3$ solid solutions, Journal of Solid State Chemistry 166 (2002) 81–90.

[17] Y. Yamamoto, T. Sekino, T. Kusunose, T. Nakayama, Y. Morimoto, S. Miyazawa, K. Niihara, The formation of self-organized regular array microstructure derived from structural anisotropy of phase M solid-solution, Journal of Crystal Growth 264 (2004) 445–451.

[18] B.W. Li, M. Osada, T.C. Ozawa, R. Ma, K. Akatsuka, Y. Ebina, H. Funakubo, S. Ueda, K. Kobayashi, T. Sasaki, Solution-based fabrication of perovskite nanosheet films and their dielectric properties, Japanese Journal of Applied Physics 48 (2009) 09KA15.

[19] B.W. Li, M. Osada, T.C. Ozawa, Y. Ebina, K. Akatsuka, R. Ma, H. Funakubo, T. Sasaki, Engineered interfaces of artificial perovskite oxide superlattices via nanosheet deposition process, ACS Nano 4 (2010) 6673–6680.

[20] R.S. Roth (ed.), Phase Equilibria Diagrams, American Ceramic Society, Westerville, OH, 11, 1995, pp. 231–232.

[21] J.A. Garcia, M.E. Villafuerte-Castrejon, J. Andrade, R. Valenzuela, A. R. West, New rutile solid solutions, $Ti_{1-4x}Li_xM_{3x}O_2$: M=Nb, Ta, Sb, Materials Research Bulletin 19 (1984) 649–654.

[22] R.I. Smith., A.R. West, Characterization of an incommensurate LiTiNb oxide, Materials Research Bulletin 27 (1992) 277–285.

[23] P.H. Xiang, Y. Kinemuchi, K. Watari, Synthesis of layer-structured ferroelectric Bi_3NbTiO_9 plate-like seed crystals, Materials Letters 59 (2005) 1876–1879.

[24] M.W. Anderson, J.R. Agger, N. Hanif, O. Terasaki, Growth models in microporous materials, Microporous and Mesoporous Materials 48 (2001) 1–9.